Research Article

Roof Stability of Rectangle Coal Roadway: In Light of Calculation of Compressive Bar Stability

Ma Shou-Long,[1,2] Gao Linsheng [ID],[3] Yang Yue [ID],[3] Peng Rui,[3] and Zhao Qifeng[3]

[1]School of Civil Engineering and Architecture, Anhui University of Science and Technology, Huainan, Anhui 232001, China
[2]China Coal Xinji Energy Co., Ltd, Huainan, Anhui 232001, China
[3]School of Safety Engineering, North China Institute of Science and Technology, Beijing 101601, China

Correspondence should be addressed to Gao Linsheng; gaolinsheng@ncist.edu.cn

The roadway roof is a key factor to the roadway stability. The analysis of roof stability is mainly based on numerical calculation and on-site observation, while the basic theory of the bearing mechanism is relatively weak. We have founded a critical pressure calculation model, on the theory of compressive bar, for the rectangle coal roadway stability. The model has been tested and verified on accuracy and feasibility while applied on a roadway case. The critical pressure for roof stability and roof bending moment and deflection under combined axial and lateral load was deduced using the theory of compressive bar stability. The numerical calculation verified the feasibility of numerical modeling of stability of compressive bar using FLAC3D, and the influence of the background ambient horizontal stress and the parameters of the contact surface to the roof stability were further studied. The result turns out that some factors lead to a higher instability tendency, including higher horizontal stress, higher cohesion force, and larger internal friction angle on the coal-rock interface and lower cohesion force and smaller friction angle on the rock-rock interface. The results contribute to bearing mechanisms of roadway roof stability, ground pressure and strata control theory and application, and design of bolting support.

1. Introduction

In the classic study of surrounding rock stability, the self-bearing capacity is usually neglected. The anchor bolt is found to hang rocks or provide support resistance to the roadway surface rock. In line with the development of bolting technology, the self-bearing capacity has been attracting more and more attention. Researchers and engineers realize that the surrounding rock is the main bearing body, while the support system is the secondary bearing body.

With the influence of rock lithology and mechanical characteristics, ground pressure, and engineering condition, most roadways are damaged to deform severely [1–3]. Some roadways, which are affected by mining activity, have to face more severe problems to maintain the surrounding rock's stability [4–6]. With the development of surrounding rock's stability, researchers and engineers have realized that the surrounding rock plays an important role as a bearing body, which is the key to maintain the roadway's stability [7]. M. D. Salamon proposed an energy-based supporting theory, which argued that the surrounding rock interacted and deformed with the artificial support system in step. Man-chu Ronald Yeung [8] found that the long-short mixing bolting system was very important to maintain the stability of supporting system, and a radial pattern bolting was better than vertical-to-rock shape. Chen Shilin [9] argued that the surrounding rock was strong in the bearing capability, while the artificial support system was just a minor role. The ground pressure was found to relate to embedding depth, shape, and size of the roadway, rock characteristics of the surrounding rock, and the flexibility of the support system. Zhao Xingguang et al. [10] analyzed the interaction between the rock dilatation and bolting system and the constrain effect of the bolting system to the rock's swelling, finding that the anchor bolting system can retard rock expanding and

modify surrounding rock pressure effectively. Aiming at the problem of uneven and severe subsidence of the roadway roof, Chen et al. [11] analyzed the stress filed in the lateral side of the mining gob, developing process in the plastic region, and the control of the support resilience on the stress field and the plastic region, combining the method of on-site observation, theoretical analysis, and numerical analysis. Based on the analysis of the surrounding rock stress field in the high depth and mining influenced roadway, Ma Nianjie et al. [12–15] discussed the mechanical and geometrical characteristics of the formation of the surrounding plastic region under both-way and nonasymmetric pressure and the influence factors of roof stability. Furthermore, some researchers applied numeric modeling to optimize the roadway design, which promoted the quality of roadway construction [16–18].

2. Critical Pressure Calculation of the Rectangle Coal Roadway in Light of Compressive Bar Stability

2.1. Theoretical Calculation Model. While the pressure achieves or is beyond a critical value, the bar will transform from a straight equivalent state to a bended equivalent state. The mechanical model is shown in Figure 1. The deflection on a cross section with a distance x from the origin point is w, leading to a lateral pressure induced bending moment on each cross section.

2.2. Calculation Process. The bending moment of the roof is

$$M = -F_q w, \tag{1}$$

where F_q is horizontal pressure, N and q are horizontal stress in MPa, respectively, and h is roof depth in meter.

For a minor bending deflection, the approximately differential equation of flexural curve is

$$\frac{\mathrm{d}^2 w}{\mathrm{d}x^2} = \frac{M}{\mathrm{EI}}. \tag{2}$$

Substitute equation (1) into equation (2):

$$\frac{\mathrm{d}^2 w}{\mathrm{d}x^2} = \frac{-F_q w}{\mathrm{EI}}, \tag{3}$$

while

$$k^2 = \frac{F_q}{\mathrm{EI}}. \tag{4}$$

Equation (3) is rewritten as

$$\frac{\mathrm{d}^2 w}{\mathrm{d}x^2} + k^2 w = 0. \tag{5}$$

The solution of which is

$$w = R_1 \sin(kx) + R_2 \cos(kx), \tag{6}$$

where R_1 and R_2 are integration constant.

With respect to the prehypothesis that the deflection is zero at the coal rectangle roadway lateral rib where the stress is at an original level, we obtain

$$R_1 \sin(kx_q) + R_2 \cos(kx_q) = 0,$$
$$-R_1 \sin(kx_q) + R_2 \cos(kx_q) = 0. \tag{7}$$

The solution is $R_1 \sin(kx_q) = 0$ or $R_2 \cos(kx_q) = 0$, and it is demanded that

$$kx_q = \frac{n\pi}{2}, \quad (n = 0, 1, 2, \ldots,). \tag{8}$$

Then, an equation is deduced:

$$k = \frac{n\pi}{2x_q}, \quad (n = 0, 1, 2, \ldots,), \tag{9}$$

and

$$F_q = \frac{n^2 \pi^2 \mathrm{EI}}{4x_q^2}. \tag{10}$$

Because n is an integer number, the former equation gives a minimum pressure level to keep the roof stable as the following equation:

$$F_q = \frac{\pi^2 \mathrm{EI}}{4x_q^2}. \tag{11}$$

In this equation, $R_1 = 0$; therefore, the critical stress is

$$q = \frac{\pi^2 E h^2}{48 x_q^2}. \tag{12}$$

And, the critical stress under horizontal strain is

$$q = \frac{E \pi^2 h^2}{48 x_q^2 (1 - \mu^2)}. \tag{13}$$

2.3. Application of the Criterion. With respect to a roof condition, where $E = 1\,\mathrm{GPa}$, $h = 2\,\mathrm{m}$, and $\mu = 0.3$, the relationship between the critical horizontal stress and x_q can be obtained by using equation (13) and is shown in Figure 2. As shown in Figure 2, the critical horizontal stress will decline sharply with an increasing x_q. The critical horizontal stress will achieve 36 MPa while the x_q is equal to 5 m. A classical roof tends to keep stable because the original rock stress is lower. However, if the lateral rib of the roadway is broken, meaning x_q is increased, and the critical horizontal stress is declined, the roof may be unstable.

3. The Bending Moment and Sinking of the Rectangle Coal Roadway under the Bending with Combined Axial and Lateral Load

The deflection of the roof is usually small, so the deflection caused by horizontal stress is neglectable. However, if the
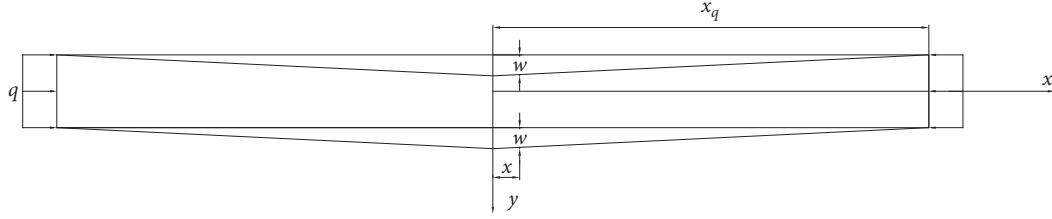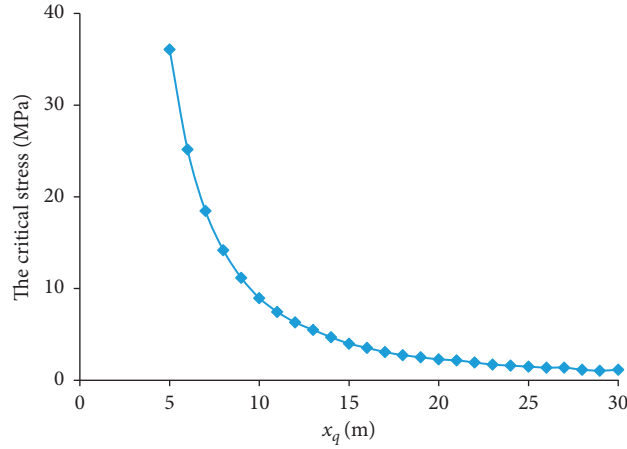
FIGURE 1: Mechanical model of roof stability considering compressive bar stability.

FIGURE 2: The relationship between critical horizontal stress and x_q.

roof deforms severely, the horizontal stress will cause a more severe bending and deformation. With respect to this condition, the horizontal and vertical stress needs to consider together, which is called bending with combined axial and lateral load in the mechanics of materials' concept. The mechanics model is shown in Figure 3.

The differential equation of the deformation curve is

$$\mathrm{EI}\frac{d^2 w}{d^2 x} = M = z_1 + z_2 x^2 + z_3 x^4 - F_q w. \qquad (14)$$

In this equation, for the roof layer No. 1, $z_1 = K_{h4}, z_2 = -(c_1/2)$, and $z_3 = -(a_1/12)$, for the roof layer No. 2 to $n{-}1$, $z_1 = K_{h7j}, z_2 = -(c_{i+1} - c_i/2)$, and $z_3 = -(a_{i+1} - a_i/12)$, and, for the roof layer No. n, $z_1 = K_{h7n}, z_2 = -(\gamma H - c_i/2)$, and $z_3 = (a_{n-1}/12)$, respectively.

Applying equation (4) to equation (14), we obtain

$$\frac{d^2 w}{d^2 x} + k^2 w = \frac{z_1 + z_2 x^2 + z_3 x^4}{\mathrm{EI}}. \qquad (15)$$

The solution of equation (14) is

$$w = R_3 \sin(kx) + R_4 \cos(kx) + \frac{z_3}{F_q} x^4$$
$$+ \left(\frac{z_2 k^2 - 12 z_3}{F_q k^2}\right) x^2 + \frac{z_1}{F_q} - 2\left(\frac{z_2 k^2 - 12 z_3}{F_q k^4}\right), \qquad (16)$$

where R_3 and R_4 are integral constants.

Apply the boundary condition that $R_3 = 0$; then, the first derivative of the deflection is

$$\frac{dw}{dx} = -k R_4 \sin(kx) + 4\frac{z_3}{F_q} x^3 + 2\left(\frac{z_2 k^2 - 12 z_3}{F_q k^2}\right) x. \qquad (17)$$

At the same time, for the rotation angle at x_q which is zero, we obtain

$$R_4 = \frac{1}{k \sin(k x_q)}\left[4\frac{z_3}{F_q} x_q^3 + 2\left(\frac{z_2 k^2 - 12 z_3}{F_q k^2}\right) x_q\right]. \qquad (18)$$

The sinking of roof and its second derivative are

$$w = \left[4\frac{z_3}{F_q} x_q^3 + 2\left(\frac{z_2 k^2 - 12 z_3}{F_q k^2}\right) x_q\right]\frac{\cos(kx)}{k \sin(k x_q)} + \frac{z_3}{F_q} x^4 + \left(\frac{z_2 k^2 - 12 z_3}{F_q k^2}\right)\left(x^2 - \frac{2}{k^2}\right) + \frac{z_1}{F_q}$$

$$\frac{d^2 w}{d^2 x} = \frac{M}{EI} = -\left[4\frac{z_3}{F_q} x_q^3 + 2\left(\frac{z_2 k^2 - 12 z_3}{F_q k^2}\right) x_q\right]\frac{k \cos(kx)}{\sin(k x_q)} + 12\frac{z_3}{F_q} x^2 + 2\left(\frac{z_2 k^2 - 12 z_3}{F_q k^2}\right), \qquad (19)$$
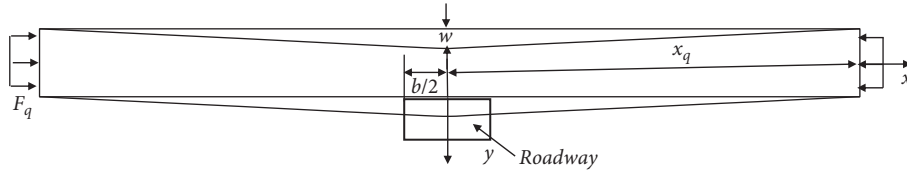
FIGURE 3: Mechanical model of the vertical and horizontal bending.

while F_q will be approaching the critical pressure ($\pi^2 EI/x_q^2$), the $\sin(kx_c)$ will be reaching infinitely small, and the roof sinking will be reaching infinitely large. The results turn out that while the horizontal approaches a critical stress, the roof will be instable even under small load. Applying the result on the combined axial and lateral stress, the modulus of elasticity E was replaced with ($E/(1 - \mu^2)$); then, the roof sinking and bending moment can be calculated.

4. Calculation of the Roof Stability considering Original Ambient Horizontal Stress and Contact Surface Parameters Based on the Compressive Bar Model

4.1. The Stability of the Compressive Bar Verified by FLAC3D. The FLAC3D has been applied and verified in the geotechnical engineering, while the application in the compressive bar model need to be further verified. In this section, the results of the FLAC3D and theoretical calculation are compared to find the feasibility of FLAC3D to calculate the roof stability.

In the FLAC3D application, a long-thin bar model was set up to simulate the roof beam structure. The model size was $100 \times 1 \times 1$ m, in 1500 cell, under even load of 1 kPa, and the bilateral constrain condition is shown in Figure 1. The model is an elastic structure unit, with the Young modulus and Poisson's ratio 10 GPa and 0.2, respectively. The roof deflection of the roof is shown in Figure 4. Note that the condition of convergence is the ratio of the maximum unequal force and internal force being 1e−6, rather than 1e−5, and the large deformation pattern was applied. As shown in Figure 4, from the bilateral stress being 0.8 MPa, deflection start to accelerate increasing. This result is similar with the theoretical calculation result, which is 0.82 MPa. Therefore, the compressive bar model using FLAC3D is proved to feasible.

4.2. Roof Stability Influenced by Original Ambient Horizontal Stress and Contact Surface Parameters Based on the Compressive Bar Model

4.2.1. Numerical Calculation Model. The calculation mode was set up in the FLAC3D application, with the presetting condition similar with the theoretical analysis. The differences are as follows. The roof load was evenly 20 MPa, the roadway width was 6 m, the calculation was under a large deformation patter, and the roof layer composition and layer-layer contact condition were different, which is shown in Table 1.
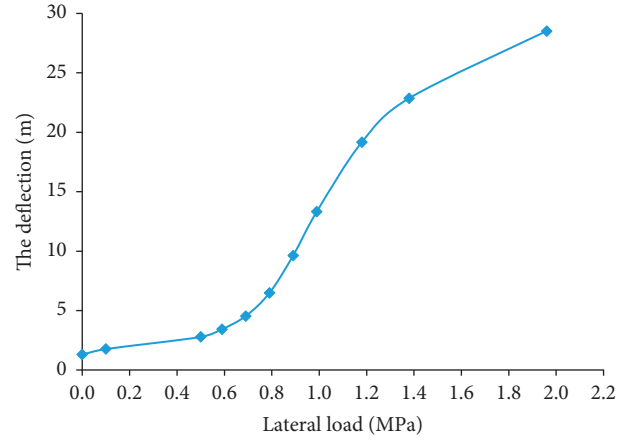

FIGURE 4: Deflection of the compressive column in FLAC3D.

4.2.2. The Influence of Horizontal Stress on Roof Stability. The roof sinking under original ambient horizontal stress of 20, 30, and 40 MPa is shown in Figure 5. Considering Figure 5 results and theoretical numerical calculation, the roof sinking was small (0.106 m and 0.115 m) with the horizontal stress 20 and 30 MPa, respectively. The roof sinking reached 0.960 m, while the horizontal has reached 40 MPa. The critical stress obtained by the theoretical numerical calculation was small, for the influence of neighboring coal seam was neglected.

The vertical stress, horizontal stress, shear stress, and interface slip under different original ambient horizontal stresses are shown in Figures 6–9. While the original ambient horizontal stress was 40 MPa, the roof sank significantly, and the horizontal and shear stress at the sinking area were abnormal. In order to show the comparison of the roof stress clearer under different original ambient horizontal stresses and interface parameters, the abnormal part was removed, and the surrounding stress of the left main part was compared. The shape of the roadway is rectangle, rather than circle. As shown in Figures 6–9, the vertical stress and shear stress shows similar pattern under different original ambient horizontal stresses. With the increase of the original ambient horizontal stress from 20 MPa to 40 MPa, the horizontal stress increased by around 10 MPa, and the interface slip scale increased.

4.2.3. The Influence of Interface Parameters on Roof Stability. As analyzed in the previous section, the roof stability is related to the interface slip. Therefore, the influence of the interface parameters on the roof stability is analyzed. The

TABLE 1: Properties of surrounding rock and interface considering compressive bar stability.

Name	Thickness (m)	Density (kg/m^3)	Cohesion (MPa)	Angle of internal friction (°)	Modulus of elasticity (GPa)	Poisson's ratio	Normal stiffness (GPa)	Tangential stiffness (GPa)
The roof layer no. 3	22	2500	—	—	10	0.2	—	—
The roof layer no. 2	0.5	2500	—	—	1	0.3	—	—
The roof layer no. 1	0.5	2500	—	—	1	0.3	—	—
Floor	23	2500	—	—	10	0.2	—	—
Coal seam	4	1300	1	25	4	0.3	—	—
Interface	—	—	0.1	10	—	—	556	556

(a)

(b)

(c)
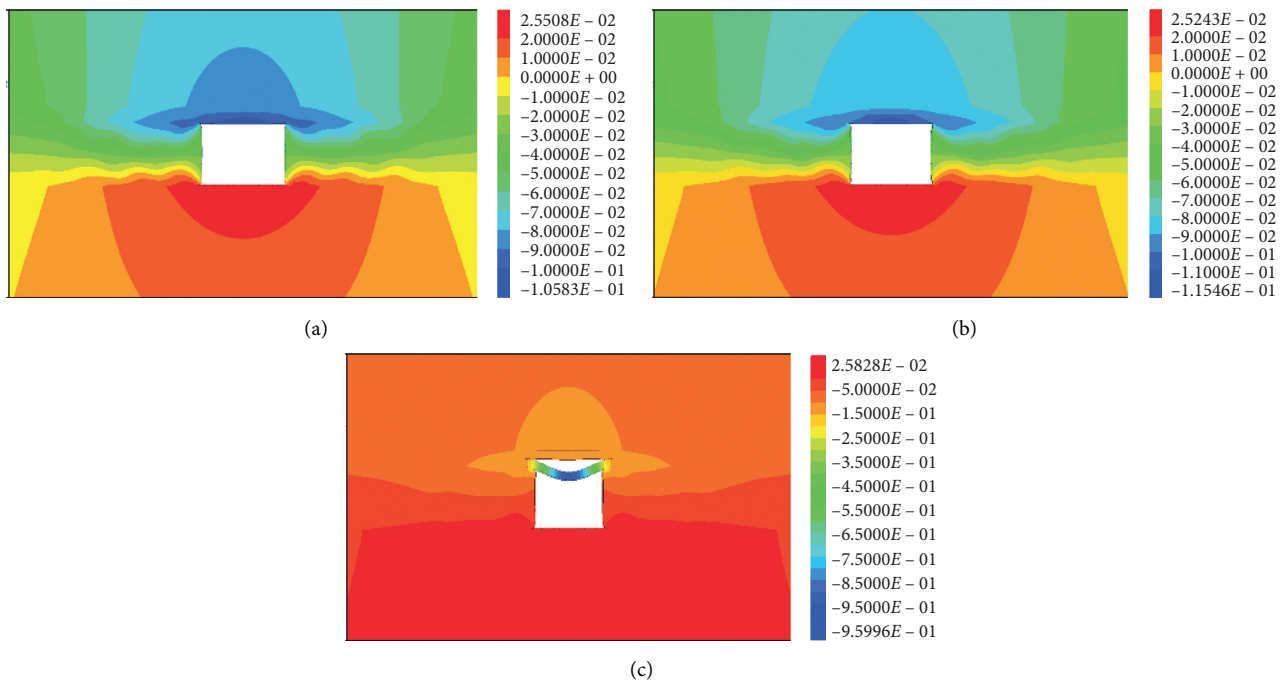
FIGURE 5: Roof sag of different horizontal stresses: (a) 20 MPa, (b) 30 MPa, and (c) 40 MPa.

immediate roof contacts with coal seam and upper layer roof. The roof-coal interface forced the roof toward roadway, while the roof-upper layer interface forced the roof toward opposite. In order to analyze the influence of the interface to the roof stability, interface parameters were changed to test the roof stability. While the system was loaded 40 MPa of horizontal stress, the roadway sinking under different cohesion force and internal friction angle are shown in Figures 10 and 11. As shown in the figures, the roof sinking increased and the more instability was observed, while the cohesion force increased from 0.1 MPa to 2 MPa. The explanation of which is that the force on the roof-coal interface forces the roof toward the roadway, so a higher cohesion force leads to a shear force. The internal friction angle showed similar influence with the cohesion force. As a conclusion, a larger cohesion force and internal friction angle lead to a less stable coal roadway roof.

Note that the previous analysis is based on the compressive bar stability theory. While the roof is deforming significantly, the horizontal force causes further roof sinking. However, the sinking of roadway roof is quite small because of the high cohesion force and internal friction angle, and large deformation and instability of roof may not happen. With a pre-setting condition of 40 MPa, the roof sinking under different cohesion forces and internal friction angles are shown in Figures 12 and 13. As shown in figures, as the cohesion force at the rock-rock interface increased from 0.1 MPa to 2 MPa, roof sinking reduced significantly. The explanation is that the cohesion force pushes the roof opposite to the roadway, so a higher cohesion force leads to a higher shear force, and a higher horizontal force is opposite to the roadway. The internal friction angle at the rock-rock interface showed a similar pattern. As a conclusion, a higher cohesion force and larger internal friction angel at the rock-rock interface lead to a more stable.
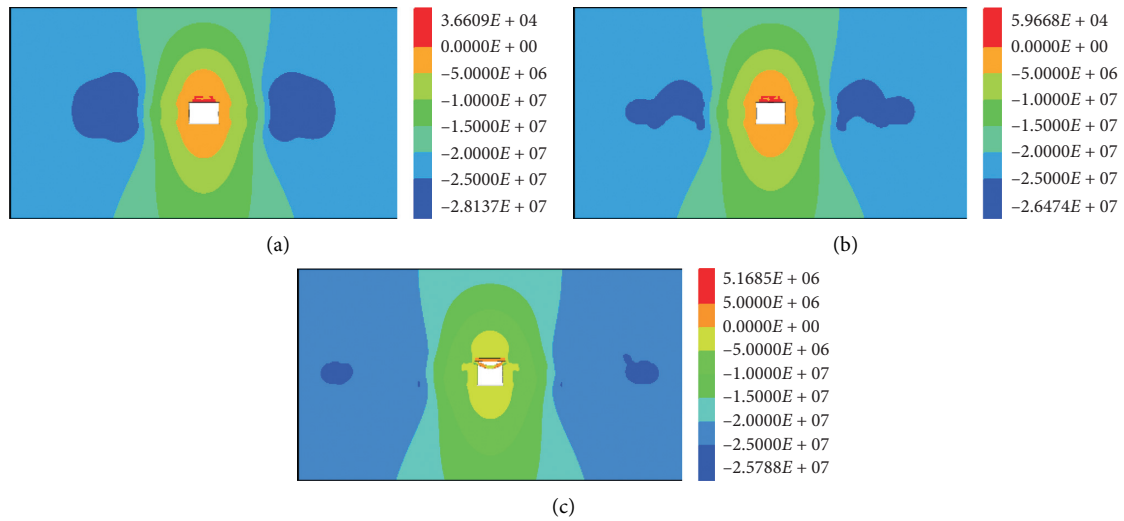
FIGURE 6: Vertical stress of roof of different horizontal stresses: (a) 20 MPa, (b) 30 MPa, and (c) 40 MPa.
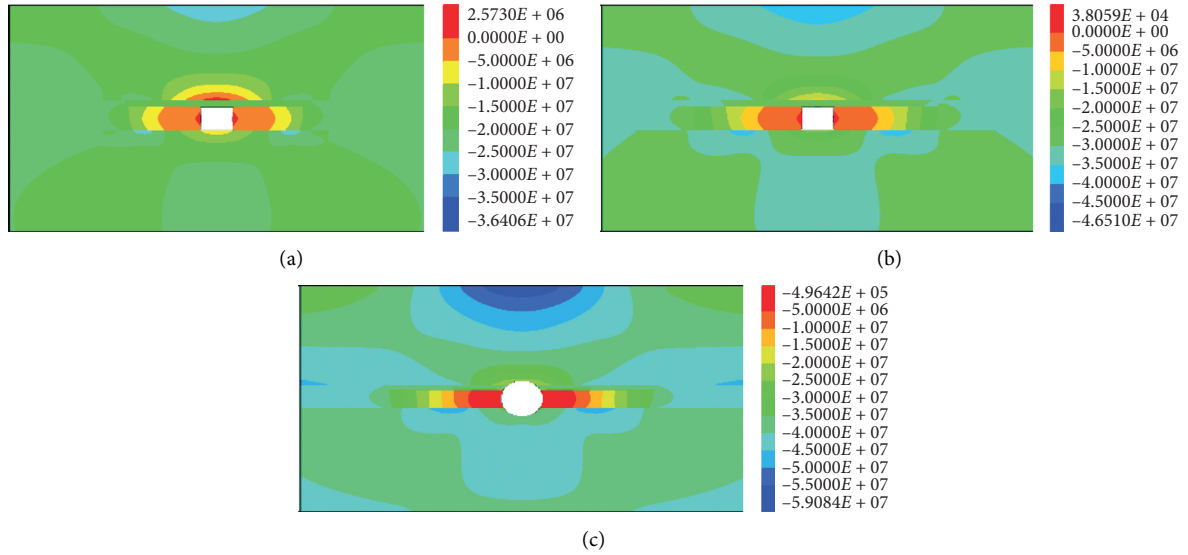

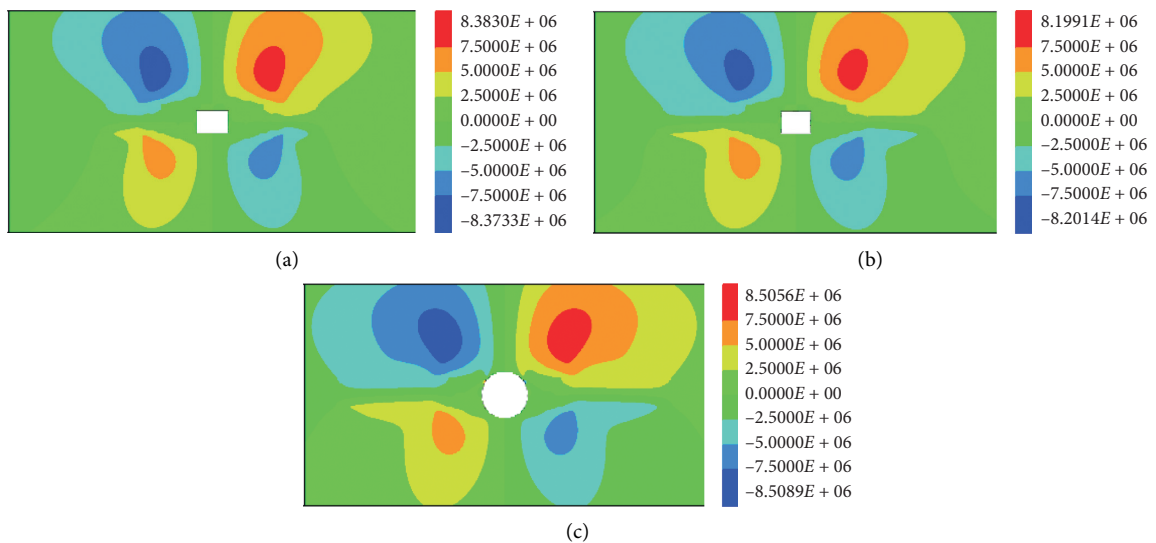FIGURE 7: Horizontal stress of roof of different horizontal stresses: (a) 20 MPa, (b) 30 MPa, and (c) 40 MPa.

FIGURE 8: Shear stress of roof of different horizontal stresses: (a) 20 MPa, (b) 30 MPa, and (c) 40 MPa.
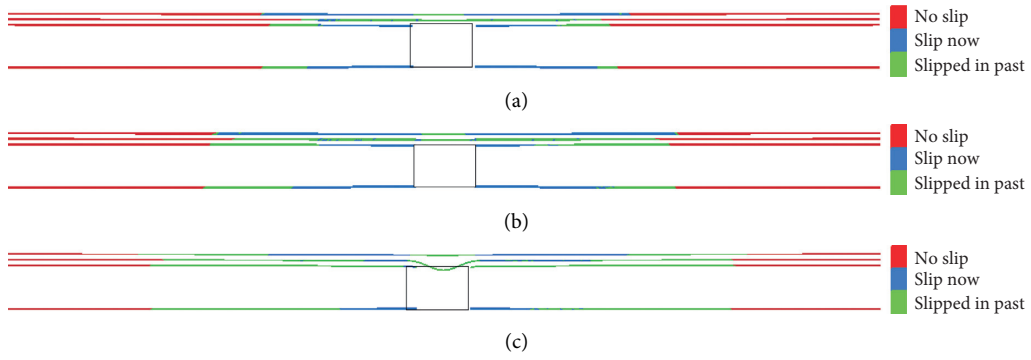
(a)

(b)

(c)

FIGURE 9: Interface slip of different horizontal stresses: (a) 20 MPa, (b) 30 MPa, and (c) 40 MPa.
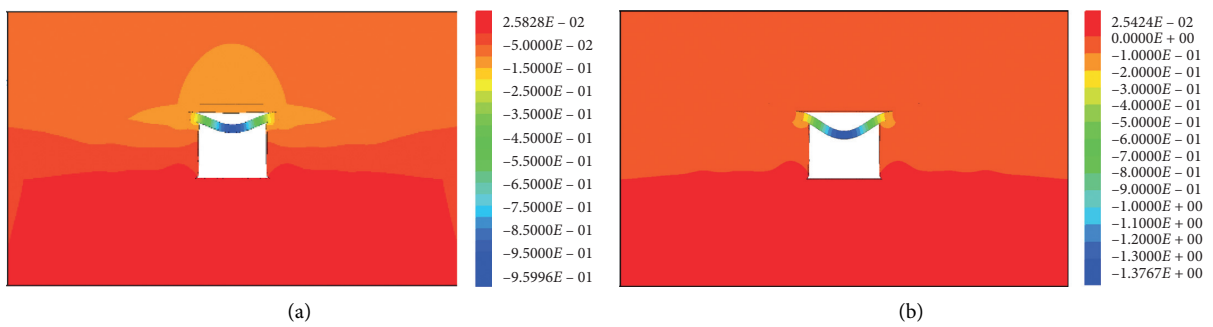

(a)

(b)

FIGURE 10: Roof sag of different rock-coal interfacial cohesion: (a) 0.1 MPa and (b) 2 MPa.
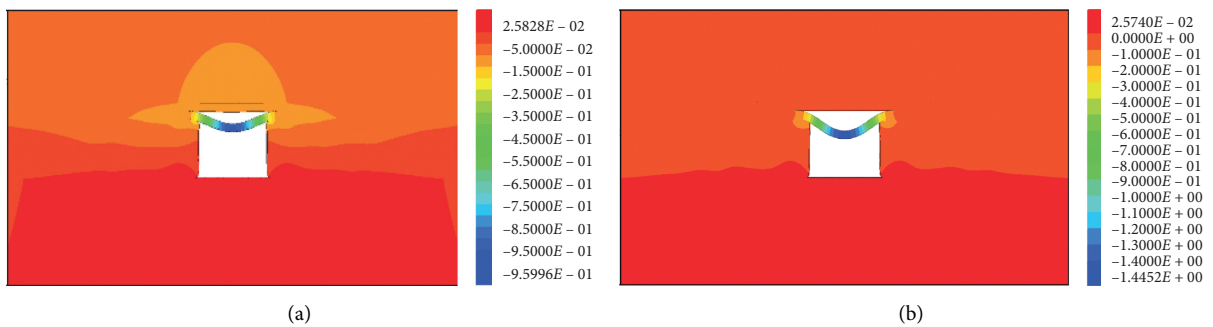

(a)

(b)

FIGURE 11: Roof sag of different rock-coal interfacial friction angles: (a) 10° and (b) 20°.

(a)

(b)

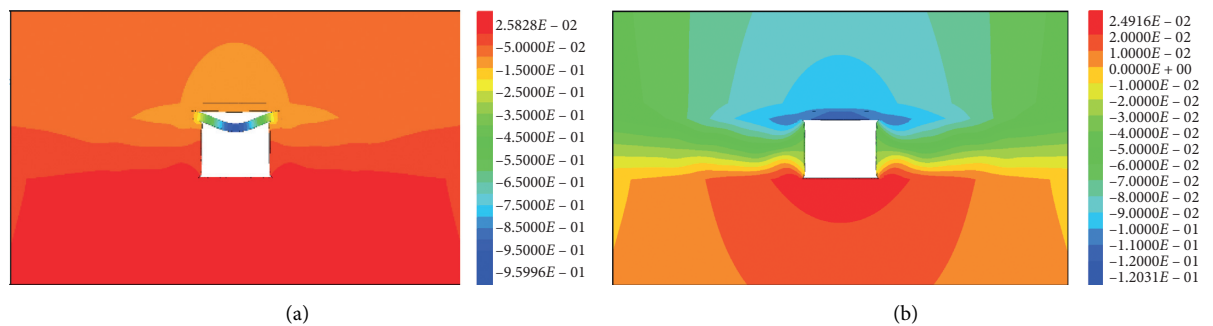FIGURE 12: Roof sag of different rock-rock interfacial cohesion: (a) 0.1 MPa and (b) 2 MPa.

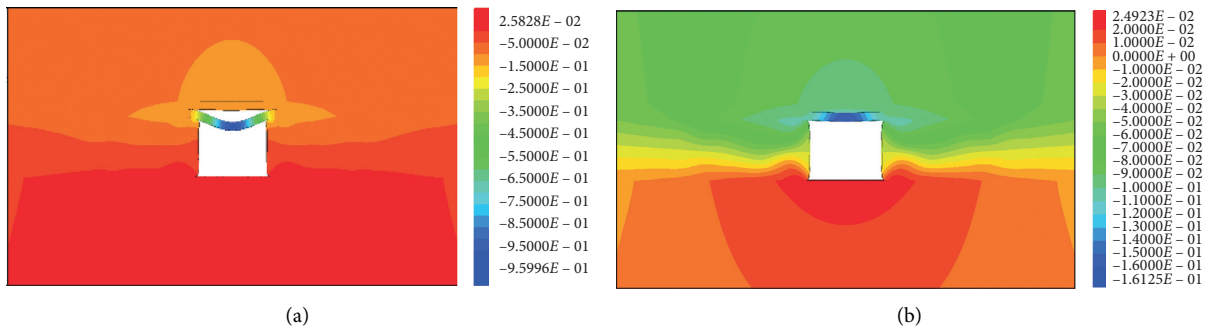(a)   (b)

FIGURE 13: Roof sag of different rock-rock interfacial friction angle: (a) 10° and (b) 20°.

Combining the Figures 12 and 13, it is concluded that the roof stability is related not only to the original ambient horizontal stress but also to the shear load from the neighboring layers. Less area of the coal-rock interface and larger area of rock-rock interface are beneficial to the roof stability. The critical pressure calculated using previous theoretical model did not take the shear stress into consideration of the roof stability. Therefore, the theoretical model is applicable while the influence of the contacting parameters is small. In the previous model, the roadway is not supported artificially, which is similar to the stained condition of floor. While the floor large deformation floor heave usually happens, and this research reveals the mechanism of floor heave, which is useful in the floor heave control.

5. Conclusions

(1) A calculation model of critical pressure for the roadway roof stability was deduced based on the compressive bar theory; then, the solution accuracy and feasibility were verified using living examples.

(2) The roof bending moment and deflection under the combined axial and lateral load was calculated.

(3) The calculation result verified the feasibility on the using of FLAC3D on the compressive bar instability. Then, the influence of original ambient horizontal stress and interface parameters on the roof stability were analyzed. The results turn out that the roof instability may be caused by higher horizontal stress, higher cohesion force, and larger internal friction angel at the coal-rock interface and lower cohesion force and smaller internal friction angle at the rock-rock interface.

Data Availability

The data used to support the findings of this study are available from the corresponding author upon request.

Conflicts of Interest

The authors declare that they have no conflicts of interest regarding the publication of this paper.

Acknowledgments

References

[1] H. Xie, F. Gao, J. Yang et al., "Quantitative definition and investigation of deep mining," *Journal of China Coal Society*, vol. 40, no. 1, pp. 1–10, 2015.

[2] M. He, H. Xie, S. Peng et al., "Study on rock mechanics in deep mining engineering," *Chinese Journal of Rock Mechanics and Engineering*, vol. 24, no. 16, pp. 2803–2813, 2005.

[3] Y. He, L. Han, S. Peng et al., "Some problems ofrock mechanics for roadways stability in depth," *Journal of China University of Mining & Technology*, vol. 35, no. 3, pp. 288–295, 2006.

[4] X. Sun, J. Yang, and W. Cao, "Research on space-time action rule of bolt-net-anchor coupling support for deep gateway," *Chinese Journal of Rock Mechanics and Engineering*, vol. 26, no. 5, pp. 895–900, 2007.

[5] J. Bai and C. Hou, "Control principle of surrounding rocks in deep roadway and its application," *Journal of China University of Mining & Technology*, vol. 35, no. 2, pp. 145–148, 2006.

[6] B. Jiang, Q. Zhang, Y. He et al., "Elastoplastic analysis of cracked surrounding rocks in deep circular openings," *Chinese Journal of Rock Mechanics and Engineering*, vol. 26, no. 5, pp. 982–986, 2007.

[7] C. Carranza-Torres, "Analytical and numerical study of the mechanics of rockbolt reinforcement around tunnels in rock masses," *Rock Mechanics and Rock Engineering*, vol. 42, no. 2, pp. 175–228, 2009.

[8] R. Y. Man-chu, "Application of shi's discontinuous deformation analysis to the study of rock behavior," Dissertation, Department of Civil Engineering College of Engineering University of California Berkeley, Berkeley, CA, USA, 1991.

[9] S. Chen, Q. Qian, and M. Wang, "Problems of deformation and bearing capacity of rock mass around deep buried tunnels," *Chinese Journal of Rock Mechanics and Engineering*, vol. 24, no. 13, pp. 2203–2210, 2005.

[10] X. Zhao, M. Cai, M. Cai et al., "Mutual influence between shear dilatation of rock mass and rebar support around underground excavation," *Chinese Journal of Rock Mechanics and Engineering*, vol. 29, no. 10, pp. 2056–2062, 2010.

[11] L. I. Chen, T. Huo, W. U. Zheng et al., "Mechanism and stability control of nonuniform and violent deformation of

dynamic pressure roadway roof," *Journal of Central South University (Science and Technology)*, vol. 51, no. 5, pp. 1317–1327, 2020.

[12] N. Ma, X. Zhao, Z. Zhao et al., "Stability analysis and control technology of mine roadway roof in deep mining," *Journal of China Coal Society*, vol. 40, no. 10, pp. 2287–2295, 2015.

[13] N. Ma, L. I. Ji, and Z. Zhao, "Distribution of the deviatoric stress field and plastic zone in circular roadway surrounding rock," *Journal of China University of Mining & Technology*, vol. 44, no. 2, pp. 206–213, 2015.

[14] X. Guo, N. Ma, X. Zhao et al., "General shapes and criterion for surrounding rock mass plastic zone of round roadway," *Journal of China Coal Society*, vol. 41, no. 8, pp. 1871–1877, 2016.

[15] L. I. Ji, N. Ma, and Z. Ding, "Heterogeneous large deformation mechanism based on change of principal stress direction in deep gob side entry and control," *Journal of Mining & Safety Engineering*, vol. 35, no. 4, pp. 670–676, 2018.

[16] X. Yang, C. Hu, J. Liang, Y. Zhou, G. Ni, and R. Huang, "A case study on the control of large deformations in a roadway located in the du'erping coal mine in China," *Advances in Materials Science and Engineering*, vol. 2019, Article ID 9628142, 13 pages, 2019.

[17] B. Shen, "Coal mine roadway stability in soft rock: a case study," *Rock Mechanics and Rock Engineering*, vol. 47, no. 6, pp. 2225–2238, 2014.

[18] L. Jiang, P. Kong, J. Shu, and K. Fan, "Numerical analysis of support designs based on a case study of a longwall entry," *Rock Mechanics and Rock Engineering*, vol. 52, no. 9, pp. 3373–3384, 2019.